2

Clustering in Heusler Alloys

N. Lakshmi[1], V. Sebastian[2], and K. Venugopalan[1]

[1] Department of Physics, Mohanlal Sukhadia University, Udaipur, 313 001 Rajasthan, India, nambakkat@yahoo.com
[2] Department of Physics, Nirmalagiri College, Nirmalagiri P.O., Kerala 670 701, India

Summary. The effect of disordering, particularly Cr clustering on the magnetic properties in bulk and nanosized Heusler alloy Fe_2CrAl has been studied using a combination of X-ray diffraction, ^{57}Fe Mössbauer spectroscopy, and DC magnetization. The structural order/disorder has been confirmed using Mössbauer spectroscopy, and the observed bulk magnetic properties have been correlated to these results. Mechanical milling of the bulk alloys result in a more even distribution of Cr, reducing the clustering and hence enhancing the bulk magnetic properties with nearly no change in the Curie temperature (T_C). Mechanical alloying of elemental Fe, Cr, and Al give rise to a highly disordered system with higher saturation moment, retentivity, and very enhanced T_C.

2.1 Introduction

Heusler alloys have been of interest since 1903 when Heusler [1] reported that ferromagnetic alloys could be made from nonferromagnetic constituents Cu, Mn, and main group elements such as Al and Sn. The ferromagnetic properties of these alloys were related to the chemical ordering and concentration of Mn atoms.

In general, there are two types of Heusler systems. The first is the full-Heusler alloy, with chemical composition X_2YZ, which crystallizes in the $L2_1$ structure [Fm3m] and consists of four sets of interpenetrating fcc planes A, B, C, and D (Fig. 2.1). The A and C sublattices with Wyckoff coordinates (0,0,0) and (1/2,1/2,1/2) are occupied by X atoms, while the B and D sublattices with coordinates (1/4,1/4,1/4) and (3/4,3/4,3/4) are occupied by the Y and Z atoms, respectively. The X atoms at the two different sublattices have the same local environment rotated by 90° with respect to the (001) axis.

The second type is the half-Heusler alloy with composition XYZ, which crystallizes in the Cl_b structure. This structure can be derived from the full Heusler structure by leaving one of the two equivalent (A,C) sites in Fig. 2.1 vacant. In both the Heusler systems, typical X-site elements are transition metal elements Cu, Pd, Au, Co, Ni, Fe, etc., Y-site elements are transition

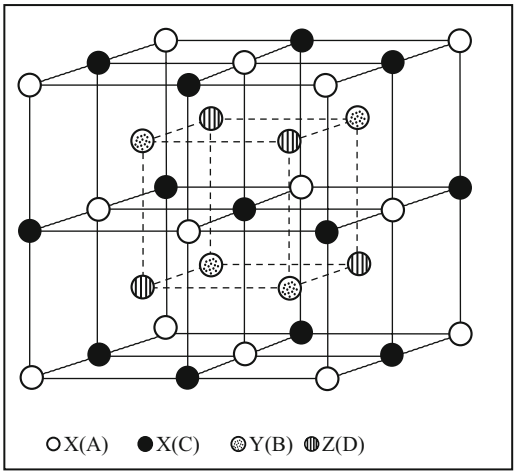

Fig. 2.1. Structure of Heusler alloys

metal elements Ti, Zr, Hf, V, Mn, Cr, etc., and Z is an s-p element like Al, Sn, In, Sb, Ge or Ga, etc. Most of these alloys, especially the X_2YZ type, are ferromagnetic at room temperature. In addition, many of these alloys also exhibit semiconducting [2], semi-metallic [3], Pauli paramagnetic [4], antiferromagnetic [5], or half-metallic [6] character.

Heusler alloys are easily amenable to partial or complete substitution of one or more of the constituent elements. This flexibility in altering the composition can be exploited to develop new materials with superior physical properties such as electrical resistivity, thermal conductivity, Seebeck coefficients, heat capacity, and magnetic properties [7]. Initial studies on Heusler alloys were limited mainly to understanding their magnetic properties using techniques such as Mössbauer spectroscopy and perturbed angular correlation (PAC).

However, in recent years, there has been a revival of interest in these alloys because of possible technological applications. A recent emerging area of technological applications of the Heusler systems is in shape memory alloys (SMA) [8, 9]. Shape memory alloys are materials that, after being strained, revert back to their original shape at a certain temperature. In Heusler systems like Ni_2MnGa, magnetic control of the structural transformation is exploited to prepare SMA systems, which are more efficient compared with conventional temperature driven SMA [10]. In recent years, Heusler systems have also been reported to be good candidates for possible applications in the emerging field of spintronics [11]. In spintronics systems, materials having nonequilibrium spin population are required for generation of spin polarization. Band structure calculations show that the gap in the minority spin band in Heusler systems can lead to 100% spin polarization of electronic states at the Fermi level [12, 13]. High Curie temperature in the range 200–1,100 K

and compatibility with compound and element semiconductors make these materials suitable for spin electronic applications.

The physical properties of Heusler alloys are dependent, to a large extent, on the degree of disorder. Although many of the Heusler alloys are chemically well-ordered, chemical disorder of various degrees can coexist in these systems, depending on the constituent elements and heat treatment given to prepare these alloys. In general, ordering is easily possible in Heusler alloys X_2YZ with Pd as X. It is observed that there is more of a tendency for disorder in Co-based alloys when compared with Pd-based alloys, especially if Z site elements are Sn or Al [14]. When X is Fe, the tendency for disorder is greater. It is now well known that iron-based transition metal alloys show a great sensitivity to environmental effects [15]. For instance, Cr, Co, or V in Fe-Al or Fe-Si systems shows definite site preference even in the presence of disorder. Such preferential occupation of the different sites gives rise to clustering effects, which influence the magnetic properties of these systems. Such clustering has been observed in different Heusler systems with $(Fe_{1-x}V_x)_3Al$ [16] being a good example. Theoretical investigation [17] of atomic disorder-effects on half metallicity of the full-Heusler alloy $Co_2(Cr_{1-x}Fe_x)Al$ shows that disorder between Cr and Al does not significantly reduce the spin polarization while disorder between Co and Cr contributes to a considerable reduction of the spin polarization. Thus, the type of atomic disorders in Heusler systems play a crucial role in determining the spin polarization and hence their utility as spin injection sources.

Atomic disorders and clustering effects also greatly influence the magnetic properties of Heusler alloys [18, 19]. Previous studies on bulk Fe_2CrAl using the Mössbauer effect have shown that even in the presence of fairly good chemical ordering, clustering of Cr influences the microscopic magnetic properties [14, 18, 20]. Moreover, on reduction in the grain size to the nanoscale, vastly different magnetic properties are expected, as, for example, in the case of Al-rich, Fe-Al systems [21]. Coupled with the ease of tailoring of magnetic properties in Heusler systems by simple substitution – wholly or partially – of constituents, change in the magnetic properties due to induced disorder as well as reduction in the grain size can give rise to a whole new class of magnetic nanosystems with improved magnetic properties like enhanced saturation magnetization and high Curie temperatures.

The present study has therefore been undertaken to better understand the effect of clustering and disorder on the magnetic properties of iso-structural full Heusler system Fe_2CrAl. The study also aims to investigate the effect of nanostructuring on the formation of clusters and the consequent changes in the bulk and microscopic magnetic properties of this Heusler alloy. The magnetic properties of nanostructured Fe_2CrAl alloys prepared through mechanical milling and mechanical alloying are compared with that obtained from the study of a bulk alloy prepared through arc melting. The nanosized samples prepared through ball milling are expected to be more disordered and could lead to an enhancement in the magnetic properties compared to the bulk alloy.

Although mechanical milling and mechanical alloying lead to nanostructured alloys of the same nominal composition, the resultant alloys can have different microstructural and magnetic properties. This chapter reports the results of a comparative study of a bulk, mechanically milled (MM) and mecahnically alloyed (MA) Fe_2CrAl, characterized using X-ray diffraction (XRD) in conjunction with Mössbauer and bulk magnetization techniques.

2.2 Experimental Methods

To prepare the bulk Fe_2CrAl alloy, stoichiometric quantities of the constituent materials of at least 99.95% purity were arc melted in argon atmosphere and annealed in vacuum ($\approx 10^{-5}$ torr) at first for 1,073 K for 72 h and further at 473 K for three days more, then cooled down to room temperature in the furnace itself. The MM and MA samples were prepared in a high-energy Spex 8000M mixer/mill using tungsten carbide balls and vials. The ball to powder ratio in both the cases was 20 : 1. The starting material for the MM sample was bulk Fe_2CrAl alloy prepared by arc melting and that for the MA sample was pure Fe, Al, and Cr taken in the required stoichiometric ratio. The MM sample was milled for 30 min and the MA sample for 15 h. Although the XRD of samples MA for 5, 10, and 15 h are nearly the same, Mössbauer spectra showed the presence of a sextet corresponding to 33 T, characteristic of α-Fe, in the 5 and 10 h alloyed samples, indicating that all the iron had not been alloyed until 15 h of milling. The sample MA for 15 h (MA) has therefore been chosen for comparison with bulk and MM samples. X-ray diffractograms of the three samples were obtained using Cu Kα radiation. Room temperature Mössbauer measurements were made using a 25 mCi ^{57}Co (Rh) source in the transmission mode. Fitting of Mössbauer spectra were made using a hyperfine field distribution program. Magnetization measurements were made on a Lake Shore 7300 Vibrating Sample Magnetometer (VSM) up to a maximum field of 1 T.

2.3 Results and Discussion

2.3.1 X-Ray Diffraction Studies

In Fm3m symmetry, Bragg reflections with nonzero structural amplitudes occur when Miller indices are all either odd or even. X-ray diffraction pattern will show three types of reflections with structure amplitudes F as follows [22]

1. h, k, l all odd, e.g., $F(1,1,1) = 4|\{(f_A - f_C)2 + (f_B - f_D)2\}1/2|$
2. h, k, l all even, which can be realized by two different conditions, which are

- $(h + k + l)/2 = 2n + 1$, e.g., $\mathrm{F}(200) = 4|f_\mathrm{A} - f_\mathrm{C} + f_\mathrm{B} - f_\mathrm{D}|$
- $(h + k + l)/2 = 2n$, e.g., $\mathrm{F}(220) = 4|f_\mathrm{A} + f_\mathrm{C} + f_\mathrm{B} + f_\mathrm{D}|$

In the above expressions, f_A, f_C, f_B, and f_D are the average scattering factors of atoms at the corresponding lattice sites. Reflections for which $(h + k + l)/2 = 2n$ are the principal reflections. As seen from the above expression, all the average scattering factors simply add up and so any interchange in positions will not affect the structure amplitude F in this case. Thus, the intensity of the principal reflections are unaffected by the state of chemical ordering. However, the other two groups representing superlattice reflections are sensitive to chemical ordering. Measurement of the intensities of the superlattice reflections relative to that of the principal reflection can give the type of chemical disordering. Johnston and Hall [23] and Ziebeck and Webster [24] have discussed in detail the effects of different types of disorder on the structure amplitudes of ternary alloys of the Heusler type.

Figure 2.2 shows the XRD patterns of bulk, MM, and MA samples. The Fe_2CrAl (220), (400), and (422) peaks are present in all the three samples.

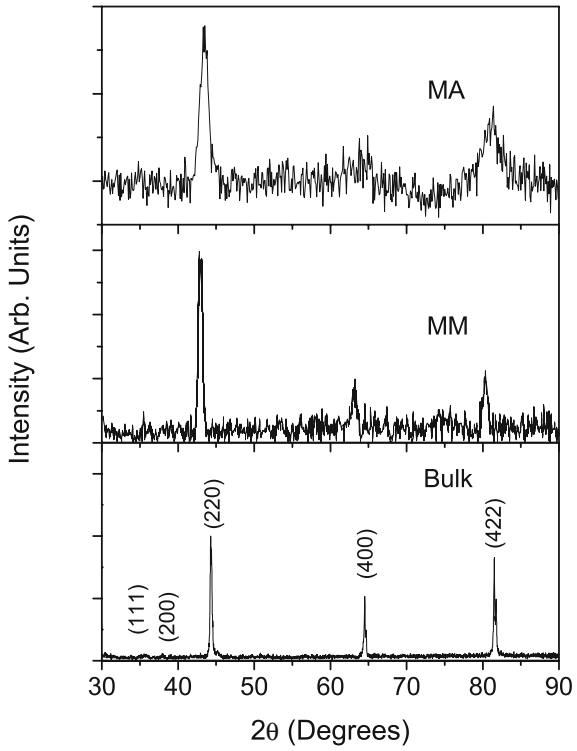

Fig. 2.2. X-ray diffraction patterns of bulk Fe_2CrAl prepared by arc melting, nanosized Fe_2CrAl prepared by high energy ball milling of the bulk sample for 30 min (MM) and 15 h MA Fe_2CrAl

The value of lattice parameter a_0 for the bulk sample is 0.5803 nm and is comparable to that reported by Zhang et al. [20] and earlier reported values [2,14]. Paduani et al. [25] have also reported similar values. Two low intensity peaks at 27.8° and 32.2° are present in the XRD spectrum of the bulk sample, which correspond to the (111) and (200) superlattice peaks.

The degree of ordering in the sample can be measured by looking at the relative intensities of these two peaks with respect to the fundamental (220) peak. These two superlattice peaks disappear for the case of randomly occupied lattice sites (A2 structure). In the case of the Heusler alloy $Co_2Mn_{1-x}Fe_xSi$, it has been pointed out that when Mn/Fe sites are randomly occupied by Mn/Fe and Si, the structure is B2 and only the (200) superlattice peak would be present, while the (111) peak vanishes [26]. When Co atoms are partly replaced by Mn/Fe atoms in $Co_2Mn_{1-x}Fe_xSi$, the intensity of the (111) superlattice peak would have a higher intensity than the (200) peak. They have also pointed out that the intensity of the (111) and (200) peaks would be equal in the case of $L2_1$ structure. Since Fe_2CrAl is also a Heusler alloy with a similar structure, the degree of ordering and the nature of antisite disorders can be determined from the study of the relative intensities of the corresponding superlattice peaks. It is seen that the relative integrated intensity of the (111) peak is 10.1% with respect to the (220) peak, which is within expected limits of error of the reported value of 10%, while the (200) peak has a relative intensity of only 1% with respect to the (220) peak. In analogy with other Heusler alloys, this indicates that even in the bulk sample, there is an appreciable degree of antisite disorder, with Cr atoms replacing Fe atoms at the Fe sites.

When the bulk sample is milled for 30 min, it is seen that the fundamental peaks are shifted to the left, indicating an expansion of the lattice. The lattice constant of the sample is 0.5951 nm, equivalent to an expansion of ≈2.5% compared with the bulk sample. High energy ball milling is known to produce lattice disorder and a high density of point defects like antisite atoms and vacancies, which leads to an expansion of the lattice [27, 28]. The relatively high value of lattice expansion in this sample points to the high density of antisite disorders. The presence of defects and vacancies in the present sample is also indicated by the decrease in intensity of the (111) superlattice peak and the disappearence of the (200) peak. The broadening of the peaks due to crystallite refinement and increase in lattice strain also contribute to the decreased intensity of these peaks. The crystallite size calculated using the Williamson–Hall [29] method shows that the crystallite size of the milled sample is ≈15 nm after 30 min of milling.

XRD spectra of the elemental powders of Fe, Cr, and Al, MA for 5, 10, and 15 h, are given in Fig. 2.3. The samples are labeled MA 5, MA 10, and MA 15 in the figure. All the three samples have similar XRD spectra, with the (220), (400), and (422) peaks corresponding to Fe_2CrAl visible in all the spectra. Since the fundamental peaks of pure Fe also lie at nearly the same 2θ values, the presence of pure Fe phase cannot be detected by XRD. However, as the hyperfine field values of pure Fe and Fe_2CrAl are very different, the presence of

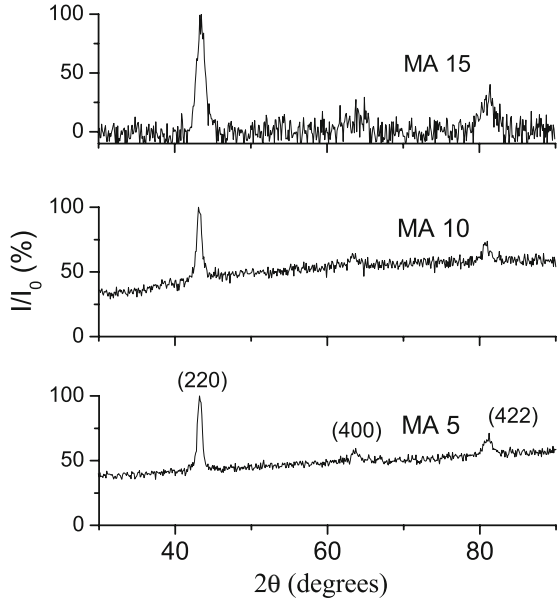

Fig. 2.3. X-ray diffraction spectra of Fe_2CrAl prepared by mechanically alloying elemental powders of Fe, Cr, and Al powders for 5, 10, and 15 h. The sample denoted as MA 15 in this figure is denoted as MA in Fig. 2.2

unalloyed Fe can be detected through Mössbauer studies. Presence of pure Fe phase is observed in the MA 5 and MA 10 samples, indicating that the alloying is not complete, whereas, Mössbauer studies on the MA 15 sample do not show evidence for the pure Fe phase. Thus, from XRD and Mössbauer studies, it can be concluded that the elemental powders have completely alloyed to form Fe_2CrAl alloy after mechanical alloying for 15 h. Therefore, only the MA 15 sample, i.e., the one MA for 15 h, referred to as MA in text, has been used for further studies.

From Fig. 2.3, it is evident that the fundamental peaks are gradually broadened with increase in MA time, indicating a reduction in the crystallite size and an increase in lattice strain. The crystallite size of the sample milled for 15 h (MA), calculated using the Williamson–Hall method is ≈8 nm. The lattice constant for this sample is 0.588 nm, corresponding to ≈1.3% expansion with respect to the bulk. However, it is smaller than that of the MM sample. The expansion of the lattice in this sample may be due to slight deviations from the stoichiometry, since the mechanical alloying process could produce other, nonstoichiometric, phases too. However, the fraction of other phases is too low since they have not been detected by XRD and Mössbauer studies. The superlattice peaks are also absent in this sample (Fig. 2.2), indicating a high degree of disorder, as is expected for alloys prepared by mechanical alloying.

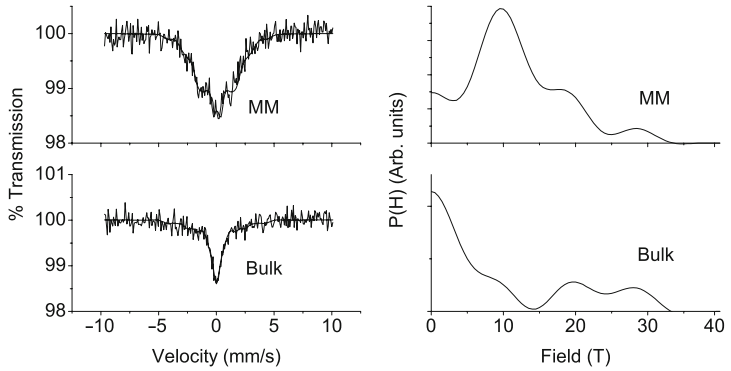

Fig. 2.4. Room temperature Mössbauer spectra and magnetic hyperfine field distributions of bulk Fe_2CrAl prepared by arc melting and nanosized Fe_2CrAl prepared by high energy ball milling of the bulk sample for 30 min (MM)

2.3.2 Mössbauer Studies

Room temperature Mössbauer spectra (Fig. 2.4) of the bulk and MM samples show the presence of a weak, unresolved magnetic sextet and a paramagnetic singlet. The isomer shift of the singlet is very near to zero in both the cases. On fitting a single sextet and singlet using discrete Lorentzians, the width of the peaks of the sextet is about two times that of natural iron. Hence, the spectra were fitted for a distribution of hyperfine fields using Windows programme [30] and the corresponding hyperfine field distribution (HFD) is also shown in Fig. 2.4. The line widths of the individual Gaussians were constrained to be equal to that of α-iron.

The hyperfine field distribution of the bulk sample consists of a dominant paramagnetic component, a component centered on 9.5 T and two higher magnetic field components of almost equal intensity (Fig. 2.4). Temperature-dependent Mössbauer studies [14] on bulk Fe_2CrAl has shown that the paramagnetic peak is present even at low temperatures. From these studies, it was concluded that the paramagnetic singlet in the bulk sample is due to Cr atoms replacing Fe at Fe sites, leading to the clustering of Cr atoms. This is consistent with the conclusions drawn from XRD studies that Fe-Cr type disorder is still present in the sample. Such antisite disorder has been observed in well-ordered samples of other Heusler alloys such as Co_2FeSi [31] also.

The magnetic hyperfine field distribution (HFD) for the bulk sample shows two high field components of almost equal intensity centered at 28.6 and 19.8 T in addition to a low field component at 9.5 T. Fe at the equivalent A and C sites in a fully-ordered Heusler structure have the same environments and so magnetic HFD of the Mössbauer spectrum of Fe_2CrAl should have only a single peak corresponding to one unique Fe site [14]. The low field peak at 9.5 T can be attributed to Fe atoms in the perfectly ordered environment.

Table 2.1. Bulk magnetic parameters of the bulk, MM, and MA samples

Sample	M_s	M_r	H_c (mT)	T_c (K)	H_{av} (T)
Bulk	1.08	0.005	0.4	298	9.9
MM	1.95	0.036	1.4	300	11.8
MA	2.24	0.332	15.9	887	18.0

Saturation magnetization (M_s) and retentivity (M_r) are in units of μ_B/formula unit. The average field (H_{av}) is obtained from Mössbauer measurements

The presence of two additional peaks in the HFD can be attributed to the Cr clustering. The clustering of Cr atoms would, in the basic $L2_1$ lattice, lead to an excess of Fe atoms being displaced from their actual positions. Thus a fraction of Fe atoms would be in an Fe_3Al-like environment. This is supported by the fact that the hyperfine fields reported for disordered Fe_3Al alloy is very close to the two high field peaks, viz. at 19.8 T and 28.6 T obtained here [32]. The overall microscopic picture obtained from Mössbauer studies is thus consistent with the conclusions drawn from XRD studies that Fe-Cr type of disorder persists in the bulk sample. However, since the integrated intensity of the peaks for the high field components are very small, the disorder in this sample can be assumed to be very small and is consistent with the (220) superlattice peak in XRD.

There is a slight increase in the average magnetic hyperfine field for the MM sample, compared with the bulk. It increases from 9.9 T for the bulk sample to 11.8 T for the milled sample (Table 2.1). On milling, the alloy becomes more disordered as indicated by the disappearance of the superlattice peaks in XRD and the increase in width of the peaks in the Mössbauer spectrum. Milling leads to a greater density of defects and vacancies in the sample, so that effects due to Cr screening and dilution effect due to Al nearest neighbors on Fe is decreased, resulting in a higher average magnetic field for the MM sample. According to the Bethe-Slater curve, an increase in the nearest neighbor distance, in the case of Fe, would lead to an increased magnetic hyperfine field [33, 34].

Mössbauer spectrum of the MM sample (Fig. 2.4) shows that the paramagnetic peak in the MM sample has a much lower intensity, which is reflected in the HFD also, despite the fact that Curie temperatures of both, the bulk and MM samples, are nearly the same. The main difference between the bulk and MM samples as observed from HFD is that the most dominant peak for the MM sample is at ≈9.8 T while it is the zero field peak for the bulk sample. The two high field peaks present in the bulk sample are also present in the MM sample. However, since the most intense peak in the HFD is at ≈9.8 T, which corresponds to the expected value for well-ordered Fe_2CrAl, it appears that the disordering produced due to milling leads to a more even distribution of Cr atoms, resulting in the disappearance of Cr clusters present in the

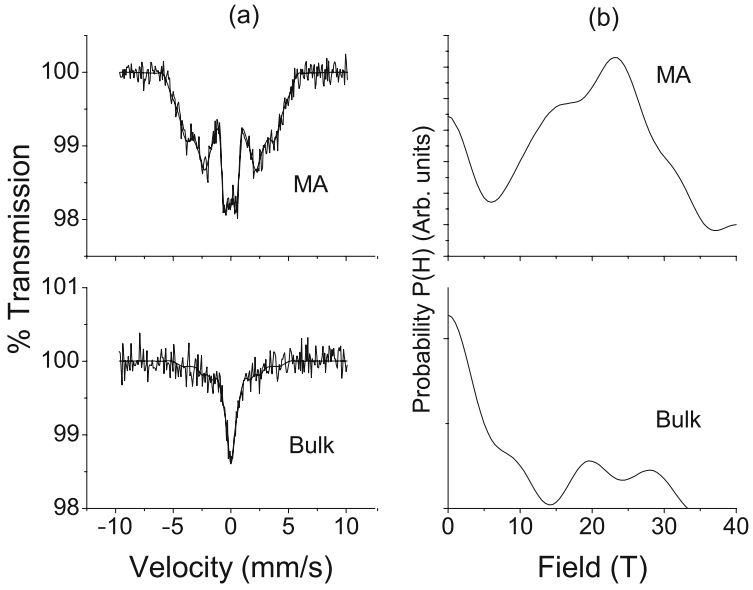

Fig. 2.5. The Mössbauer spectrum and hyperfine field distribution (HFD) of the sample MA for 15 h (MA). Mössbauer spectrum and hyperfine field distribution (HFD) of the bulk sample is also given for comparison

bulk sample. The decrease in intensity of the paramagnetic component also supports this conclusion that the Cr atoms are redistributed. Thus, hyperfine studies on bulk and milled Fe_2CrAl systems leads to the conclusion that the Fe-Cr type disorder, leading to Cr clustering is decreased on milling, although random disorder increases.

Room temperature Mössbauer spectra and the hyperfine field distributions of the MA sample is given in Fig. 2.5. The spectrum consists of a paramagnetic singlet and a more pronounced sextet. The isomer shift of the singlet is again close to zero, as in the case of the bulk sample. The Mössbauer spectrum and HFD of the bulk sample is also shown in Fig. 2.5 for comparison.

Consistent with the highly disordered nature of the sample, the Mössbauer spectrum of the MA sample is broad indicative of the distributed nature of the hyperfine fields. The MA sample has a higher ferromagnetic component, as is evident from the more prominent shoulders corresponding to the sextet.

The magnetic hyperfine field distributions of the MA sample does not show any evidence for unalloyed Fe, and is also considerably different from that of the bulk and MM samples. From the HFD, it is seen that the zero field peak corresponding to the paramagnetic part of the spectrum of the MA sample has a lower probability when compared with that of the bulk, pointing to a more random distribution of the Fe, Cr, and Al atoms. Also, the low field peak around 10.0 T, which was present in both the bulk and milled samples is

absent in the MA sample. The absence of this peak in the MA samples cannot be attributed to nanocrystallization, since in the nanosized MM sample, this peak is the most prominent. Thus, the disappearance of this peak is entirely due to the higher random disorder present in the MA systems.

Mössbauer studies therefore show that the Fe environment in the nanosized MA sample is different from that of the bulk. The MA sample has two HFD components at 23.3 T and 15.5 T. The integrated intensities of the high field peak of the MA samples around 24 T is much higher than the integrated intensity of the 28.6 T component of the bulk sample. Thus, the probability of Fe atoms in the MA samples having less than four nearest neighbor Al or Cr atoms is much higher than that for the bulk sample.

2.3.3 DC Magnetization Studies

Hysteresis loops of bulk Fe_2CrAl, MM, and MA samples obtained at 288 K are shown in Fig. 2.6. The bulk sample is weakly ferromagnetic, with low values of coercivity and retentivity (Table 2.1). On milling the bulk sample for 30 min, it is seen that both the coercivity and the retentivity increases. On the whole, milling leads to an improvement of the ferromagnetic properties, although the Curie temperature does not change appreciably for this sample. The changes in the magnetic properties of the MM sample, compared with the bulk, can be attributed to the nanosized nature of the MM sample and the consequent changes in the microstructure. Because of nanocrystallization, the fraction of atoms on the grain boundaries and interfaces increase. As seen from Mössbauer studies, there is an increase in the disorder along with a reduction of Cr clusters, leading to a reduction of the nonmagnetic contribution.

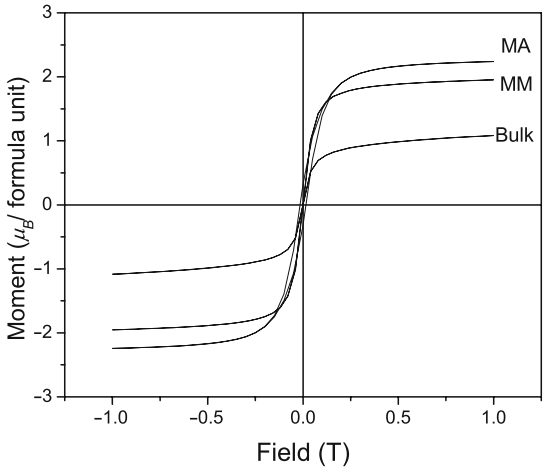

Fig. 2.6. Hysteresis loops of Bulk, MM, ASM, and ANM samples shown together to indicate the change in saturation magnetization

The hysteresis loop of the MM sample is typical of nanostructured materials with small magnetic domains [36]. The hysteresis loss in both, bulk and MM, samples is very small, indicating soft magnetic properties. The Curie temperature of the MM sample is slightly greater than that of the bulk, although the increase is not appreciable (Table 2.1). However, there is a considerable increase in the saturation magnetization of the MM sample, compared with that of the bulk, consistent with results obtained from Mössbauer studies.

The saturation moment per formula unit of the bulk is $1.08\,\mu_B$, while that of the MM sample is $1.95\,\mu_B$. The increase in saturation magnetization indicates an increase in disorder because of the milling process. During milling, the crystallite size decreases and a high density of defects are produced. XRD and Mössbauer studies also indicate a higher degree of disorder in the milled system. Such defects cause an expansion of the unit cell, leading to changes in the geometry of the atomic arrangement and interatomic distances. These changes in the lattice cause changes in the exchange interaction and hence the spin alignment. In Fe-Al systems, it has been reported that the saturation magnetization increases with lattice parameter [37]. This has been attributed to the modification of the density of states at the Fermi level.

Theoretical calculations of the density of states based on the band theory of ferromagnetism show that Fe_2CrAl falls on the Slater–Pauling curve [13]. It is predicted that well-ordered Fe_2CrAl would be a half-metallic ferromagnet and would have a total spin magnetic moment $M_t = Z_t 24$, where Z_t is the total number of valence electrons. Here it is assumed that the occupancy of the spin down bands does not change and the extra or missing electrons are taken care of by the spin up states only. In all full Heusler alloys, there are 12 occupied spin down states. Then, the total moment, which is equal to the number of uncompensated spins, is given by the total valence electrons minus two times the number of minority electrons. The total number of valence electrons in Fe_2CrAl is 25. Hence the total moment would be equal to $1\,\mu_B$/formula unit [13]. Thus, well-ordered Fe_2CrAl is expected to have a saturation moment of $1\,\mu_B$/formula unit and should exhibit half metallic properties.

However, half-metallicity has not been experimentally reported in Fe_2CrAl, since the clustering of Cr leads to the formation of highly disordered alloys [14]. In the present study, in spite of the presence of antisite disorders in the bulk sample, the saturation moment is very close to the theoretically predicted value, pointing to the possibility of realizing half metallic behavior in bulk Fe_2CrAl.

A modification of the density of states at the Fermi level due nanocrystallization and the subsequent expansion of the lattice would account for the enhancement of the total magnetic moment of the MM sample to $1.95\,\mu_B$/ formula unit from the $1.08\,\mu_B$/formula unit for the bulk sample. The saturation moment of the milled sample is also very close to an integer number ($\approx 2\,\mu_B$/formula unit) but does not conform to the $M_t = Z_t 24$ rule for Fe_2CrAl. To follow the SP behavior, theoretical calculations show that the local moment of Fe in ordered Fe_2CrAl is almost zero, while Cr has a moment of $\approx 1\,\mu_B$. The

higher magnetic moment in the MM sample also implies that Fe has a higher local moment in this sample when compared with the bulk. Two simultaneous effects in the MM sample are responsible for the overall enhancement of magnetic moment in this sample. One is that the local moment of Fe atoms increases as the size decreases. The second is that the Cr clusters are reduced – as seen from Mössbauer studies, thus reducing the number of isolated Fe atoms – again contributing to an increase in the effective saturation magnetization.

The M-H loop of the MA sample is significantly different from that of the bulk and MM samples in that it exhibits enhanced bulk magnetic properties. The coercivity and the retentivity of the MA sample is much higher (Table 2.1). Although the saturation magnetization of the MA sample is very close to that of Fe, Mössbauer studies have completely ruled out the presence of unalloyed Fe in this sample. Thus, it appears that the size of the crystallites play an important role in determining the saturation moment, since the size of this sample is half that of the MM sample, while the lattice parameter is smaller. Expectedly, the degree of disorder in this system is also higher than that in the MM sample. Thus, the increase in the saturation moment in the MA sample compared with the MM sample, which is also nano sized, can be attributed to a higher disorder in addition to size effects.

Another major difference between the MA sample compared with bulk and MM samples is the dramatic enhancement in the Curie temperature (T_C) of the MA sample. Both the bulk and MM samples have Curie temperatures very close to room temperature, while the T_C of the MA sample is 887 K (Fig. 2.7). Since the MM sample, which has a Curie temperature comparable to that of the bulk, is also nanostructured, this enhancement in Curie temperature cannot be attributed to the nanocrystalline nature of the samples alone.

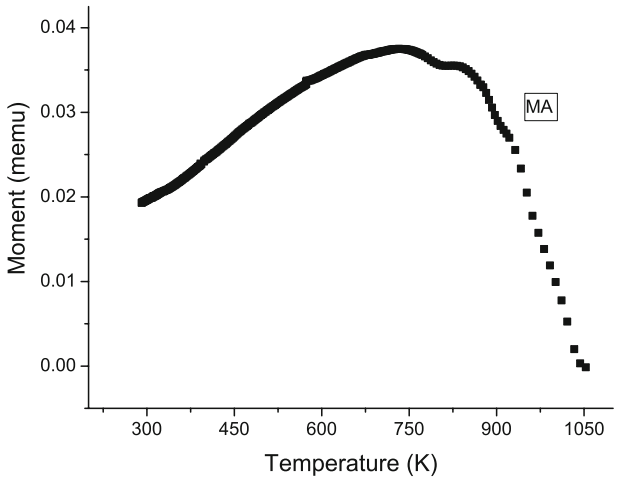

Fig. 2.7. M-T curve of nanosized Fe_2CrAl powders prepared by mechanical alloying

A comparison of the magnetic properties of MM, MA and bulk samples show that the magnetic parameters of the MA sample are the highest. Mössbauer studies show that the MA sample has a dominant high field component (≈24 T), which indicates an ^{57}Fe environment with fewer Cr and Al ions. Presumably the ferromagnetic coupling between the Fe atoms of this phase is strong and is probably enhanced due to the small grain sizes. Since the exchange stiffness is directly proportional to the Curie temperature, the dramatic increase in T_C in the MA samples indicate that the spins in these systems are more strongly aligned compared with the bulk and MM samples.

In conclusion, it is seen that the magnetic properties of nanostructured Fe_2CrAl alloys are dependent on both the size of the crystallites and on the degree of ordering in the samples. The most dramatic change is observed between the bulk and MM samples, since the enhancement in M_s is nearly 80% in the MM sample compared with that of the bulk, while the Curie temperature of both samples are nearly the same and very close to room temperature. In comparison, the saturation magnetization of the MA samples is only about 15% larger than the MM samples. However, the much higher T_C for these samples makes them better for possible use as soft ferromagnets. Also, the nearly integral values of the saturation magnetization (in units of Bohr magneton) of the samples indicate the possibility of making Fe_2CrAl alloys exhibiting half metallic properties. Although mechanical milling/alloying expectedly induces more random disorders, it is also accompanied by a reduction in Cr clustering, leading to superior magnetic properties in the nanosized alloys.

Acknowledgment

We acknowledge UGC-DRS and DST-FIST programs at the physics department, M.L. Sukhadia University, Udaipur, India.

References

1. F. Heusler, Verh. Dtsch. Pys. Ges. **5**, 219 (1903)
2. K.H.J. Bushow, P.G. Van Engen, J. Magn. Magn. Mater. **25**, 10 (1981)
3. C.S. Lue, Y.K. Kuo, Phys. Rev. B **66**, 085121 (2002)
4. K. Kobayshi, R.Y. Umetsu, R. Kainuma, K. Ishida, T. Oyamada, A. Fujita, Appl. Phys. Lett., **85**, 4684 (2004)
5. A. Ślebarski, J. Deniszczyk, W. Borgie, A. Jezicrski, M. Swatek, A. Winiarska, M.B. Maple, W.M. Yuhasz, Phys. Rev. B **69**, 155118 (2004)
6. R.A. De Groot, F.M. Mueller, P.G. van Engen, K.H.J. Bushow, Phys. Rev. Lett. **50**, 2024 (1983)
7. C.S. Lue, Y.K. Kuo, S.N. Horn, S.Y. Peng, C. Cheng, Phys. Rev. B **71**, 064202 (2005)
8. K. Ullako, J.K. Huang, C. Kantner, R.C. OHandley, V.V. Kokorin, Appl. Phys. Lett. **69**, 1996 (1996)

9. J. Marcos, A. Planes, L. Mañosa, A. Labarta, B.J. Hattink, IEEE Trans. Mag. **37**, 2712 (2001)
10. S.J. Murray, M. Marioni, S.M. Allen, OHandley, T.A. Lograsso, Appl. Phys. Lett. **77**, 886 (2000)
11. I. Zutic, J. Fabian, *Das Sarma S*, Rev. Mod. Phys. **76**, 323 (2004)
12. J.M.D. Coey, M. Venkatesan, J. Appl. Phys. **91**, 8345 (2002)
13. I. Galanakis, P.H. Dederichs, N. Papanikolaou, Phys. Rev. B **66**, 174429 (2002)
14. N. Lakshmi, K. Venugopalan, J.P. Varma, J. Phys. **59**, 531 (2002)
15. M.C. Cadeville, J.L. Moran-Lopez, Phys. Rep. **153**, 1153 (1987)
16. T.K. Nielsen, P. Klaven, R.N. Shelton, Sol. Stat. Commun. **121**, 29 (2002)
17. Y. Miura, K. Nagao, M. Shirai, Phys. Rev. B **69**, 144413 (2004)
18. N. Lakshmi, R.K. Sharma, K. Venugopalan, Hyperfine Interact. **160**, 227 (2005)
19. A. Ślebarski, J. Phys. D Appl. Phys. **39**, 856 (2006)
20. M. Zhang, E. Brück, F.R. de Boer, G. Wu, J. Magn. Magn. Mater. **283**, 409 (2004)
21. V. Sebastian, N. Lakshmi, K. Venugopalan, J. Magn. Magn. Mater. **309**, 153 (2007)
22. R.A. Dunlap, G. Stroink, Cand. J. Phys. **60**, 909 (1982)
23. G.B. Johnston, E.O. Hall, J. Phys. Chem. Solids **29**, 193 (1968)
24. K.R.A. Ziebeck, P.J. Webster, J. Phys. Chem. Sol. **35**, 1 (1974)
25. C. Paduani, W.E. Pöttker, J.D. Ardisson, J. Schaf, A.Y. Takeuchi, M.I. Yoshida, S. Soriano, M. Kalisz, J. Phys. Cond. Mat. **19**, 156204 (2007)
26. M. Kallmayer, H.J. Elmers, B. Balke, S. Wurmehl, F. Emmerling, G.H. Fecher, C. Felser, J. Phys. D Appl. Phys. **39**, 786 (2006)
27. H. Xiao, I. Baker, Acta Metall. Mater. **43**, 391 (1995)
28. L.S.J. Peng, G.S. Collins, Mater. Sci. Forum **235–238**, 537 (1997)
29. G.K. Williamson, W.H. Hall, Acta Metall. **1**, 22 (1953)
30. B. Window, J. Phys. E **4**, 401 (1984)
31. S. Wurmehl, G.H. Fecher, H.C. Kandpal, V. Ksenofontov, C. Felsr, Appl. Phys. Lett. **88**, 032503 (2006)
32. N. Lakshmi, V.K. Varma, J. Phys. Rev. B **47**, 14054 (1993)
33. U. Herr, J. Jing, R. Birringer, U. Gonser, H. Gleiter, Appl. Phys. Lett. **50**, 472 (1987)
34. U. Gonser, Hyperfine Interact. **68**, 71 (1991)
35. K. Fukamichi, Appl. Phys. Lett. **85**, 4684 (2004)
36. S. Azzaza, S. Alleg, H. Moument, A.R. Nemamcha, J.L. Rehspringer, J.M. Greneche, J. Phys. Cond. Mat. **15**, 7257 (2006)
37. X. Amils, J. Nogués, M. Suriñach, M.D. Baró, J.S. Muñoz, IEEE Trans. Magn. **34**, 1129 (1998)
38. S. Chikazumi, *The Physics of Ferromagnetism* (Clarendon, Oxford, 1997)

http://www.springer.com/978-3-540-69881-4

Advances in Nanoscale Magnetism
Proceedings of the International Conference on Nanoscale Magnetism ICNM-2007, June 25 -29, Istanbul, Turkey
Aktas, B.; Mikailov, F. (Eds.)
2009, XIV, 330 p. 203 illus., Hardcover
ISBN: 978-3-540-69881-4